Published in final edited form as:

Nature. 2017 March 09; 543(7644): 257–260. doi:10.1038/nature21387.

Reconstitution of the tubular endoplasmic reticulum network with purified components

Robert E. Powers[1,$], **Songyu Wang**[1,$], **Tina Y. Liu**[1,#], and **Tom A. Rapoport**[1,*]

[1]Howard Hughes Medical Institute and Department of Cell Biology, Harvard Medical School, 240 Longwood Avenue, Boston, MA 02115, USA

Abstract

Organelles display characteristic morphologies that are intimately tied to their cellular function, but how organelles are shaped is poorly understood. The endoplasmic reticulum (ER) is particularly intriguing, as it is comprised of morphologically distinct domains, including a dynamic network of interconnected membrane tubules. Several membrane proteins have been implicated in network formation[1–5], but how exactly they mediate network formation and whether they are all required is unclear. Here, we have reconstituted a dynamic tubular membrane network with purified ER proteins. Proteoliposomes containing the membrane-fusing GTPase Sey1p[6,7] and the curvature-stabilizing protein Yop1p[8,9] from *Saccharomyces cerevisiae* form a tubular network upon GTP addition. The tubules rapidly fragment when GTP hydrolysis of Sey1p is inhibited, indicating that network maintenance requires continuous membrane fusion and that Yop1p favors the generation of highly curved membrane structures. Sey1p also forms networks with other curvature-stabilizing proteins, including reticulon[8] and REEP[10] proteins from different species. Atlastin, the vertebrate ortholog of Sey1p[6,11], forms a GTP-hydrolysis dependent network on its own, serving as both a fusion and curvature-stabilizing protein. Our results show that organelle shape can be generated by a surprisingly small set of proteins and represents an energy-dependent steady state between formation and disassembly.

ER tubules have high membrane curvature in cross-section, which is generated by two families of conserved integral membrane proteins, the reticulons (Rtn) and REEPs (Yop1p in yeast)[8]. These proteins are required to maintain a tubular network in cells[8,9] and, upon reconstitution into liposomes, convert vesicles into tubules[9]. These proteins contain two sets of closely spaced transmembrane domains and a C-terminal amphipathic helix that may be required to induce membrane curvature[8,12]. Members of the Rtn and REEP/Yop1p families exist in all eukaryotic cells and have redundant functions in curvature-stabilization. Connecting tubules into a polygonal network depends on membrane fusion, a process

*To whom correspondence should be addressed to tom_rapoport@hms.harvard.edu.
$These authors contributed equally.
#Current address: 731 Stanley Hall, MS # 3220, University of California, Berkeley, CA 94720-3220, USA.

Author contribution

R.E.P. and S.W. performed all experiments. Initial tests of Sey1p and Yop1p co-reconstitution were performed by T.Y.L. R.E.P., S.W., and T.A.R. designed the experiments and wrote the paper. T.A.R. supervised the project. The authors declare no competing interests.

mediated by membrane-bound GTPases, the atlastins (ATL) in metazoans and Sey1p in yeast[6,11]. Proteoliposomes containing purified ATL or Sey1p undergo GTP hydrolysis-dependent fusion *in vitro*[7,11,13–15]. These dynamin-like proteins initially tether opposing membranes and then use GTP hydrolysis to cause their fusion[16]. In addition to curvature-stabilizing and fusion proteins, other factors have been implicated in ER network formation, including the lunapark protein[17–19], the Tts1/TMEM33 protein[20], the cytoskeleton, and molecular motors[21]. Here, we identify a minimal set of components needed for the formation of a tubular ER network.

We first tested whether a membrane network can be generated with the GTPase Sey1p and a single curvature-stabilizing protein, Yop1p, both derived from *S. cerevisiae*. Purified Sey1p and Yop1p (Extended Data Fig. 1) were incorporated into liposomes by "directed insertion"[11,13]. The proteins were oriented with their cytosolic domains on the outside (Extended Data Fig. 2) and used at a molar ratio that approximates their relative abundance in cells (Sey1p:Yop1p~1:10–1:20)[22]. A fraction of the vesicles floated in a Nycodenz gradient (Extended Data Fig. 3). For visualization by fluorescence microscopy, the liposomes also contained rhodamine-labeled phosphatidyl ethanolamine (rhodamine-PE). The reconstituted proteoliposomes were fusion competent, as demonstrated with a lipid-mixing assay (Extended Data Fig. 4)[11,13]. In fact, fusion was more efficient with proteoliposomes containing both Sey1p and Yop1p than with those containing only Sey1p.

Next we visualized the proteoliposomes by confocal fluorescence microscopy. In the absence of GTP, the sample consisted of small vesicles, appearing as bright dots (Fig. 1a). However, when the proteoliposomes were incubated with GTP, an extensive network of interconnected tubules was observed (Fig. 1a). Although the network displayed variable density (Extended Data Fig. 5), in most areas it looked strikingly similar to ER networks generated with extracts from *Xenopus laevis* eggs (Fig. 1b). In addition, like in extracts or intact cells[21,23], the reconstituted ER network exhibited dynamics, including the sliding of junctions along tubules and ring closure, i.e. the merging of two junctions into one (Fig. 1c; Supplementary Video 1). The network did not form with GTPγS, indicating that GTP hydrolysis by Sey1p is required (Extended Data Fig. 6a). Network formation was also dependent on both Sey1p and Yop1p. With Sey1p alone, the addition of GTP resulted in larger vesicles, but not tubules (Figs. 1d and Extended Data Fig. 6b). With Yop1p alone, only small vesicles or perhaps short tubules were observed in the absence or presence of GTP (Figs. 1e and Extended Data Fig. 6c), in agreement with previous results where tubules were observed by EM[9]. Network formation was seen with different ratios of Sey1p to Yop1p, as well as of protein to lipid (Extended Data Fig. 7). The lipid composition of the proteoliposomes did not seem to be of major importance, as networks could be generated with *Escherichia coli* or *S. cerevisiae* polar lipid extracts (Extended Data Fig. 8).

To test whether the reconstituted network contains both Sey1p and Yop1p, we generated fluorescently labeled versions of these proteins. Sey1p was tagged at the N-terminus with GFP, and Yop1p was labeled at lysine residues with Alexa647 dye. The labeled proteins were co-reconstituted into liposomes that also contained rhodamine-PE. Upon GTP addition, a network was formed that contained all three fluorescent labels (Fig. 1f). Both Sey1p and Yop1p distributed throughout the network. An even distribution of Yop1p is expected, but

Sey1p is typically enriched at three-way junctions *in vivo*[6,15]. The difference might be due to a higher Sey1p concentration in our *in vitro* system or to the absence of unknown factors that localize to junctions in cells. However, the Sey1p ortholog ATL1 is uniformly distributed throughout tubules *in vivo*[19], indicating that the fusion proteins need not be enriched at junctions.

The addition of GTPγS to a preformed network resulted in its rapid fragmentation (Fig. 2a). Within a few minutes, the network converted into small vesicles, although some larger structures were also observed. Intermediates of the fragmentation process were difficult to visualize, but we observed several cases in which long tubules broke into smaller ones (Fig. 2b; Supplementary Video 2). In addition, tubules probably shorten by shedding vesicles from their tips. These results show that network formation requires continuous membrane fusion by Sey1p to counterbalance fragmentation into small vesicles. This behavior is similar to that of ER networks generated in *Xenopus* egg extracts and tissue culture cells[19], which disassemble when ATL is inhibited.

To examine the reconstituted ER network in more detail, Sey1p and Yop1p were directly incorporated into unlabeled liposomes and the samples were analyzed by negative-stain electron microscopy (EM). When the proteoliposomes were incubated with GTP, small areas of a tubular network were seen (Fig. 3a,b; Extended Data Fig. 9a). No network was observed in the absence of GTP or when one of the two proteins was omitted (Figs. 3a–d). The areas of the network were much less extensive than those seen in the light microscope, likely because they only partially survived the harsh negative-staining protocol. The two bilayers and the lumen of the reconstituted tubules were clearly visible, confirming that three-way junctions indeed consist of fused, rather than simply tethered, membrane tubules. Most of the reconstituted tubules had a diameter of ~16 nm, similar to those formed with Yop1p alone[9]. They are significantly narrower than the tubules in normal cells, likely because the concentration of Yop1p is higher in the proteoliposomes than *in vivo*, an assumption supported by the observation that overexpression of curvature-stabilizing proteins in cells constricts ER tubules[9]. In the reconstituted tubules, Sey1p molecules were visible as small, globular objects that extended approximately 18 nm from the bilayer and were connected to the membrane via a thin stalk (Fig. 3b; Extended Data Figs. 9b,c), features and dimensions that are in agreement with the crystal structure of Sey1p[15]. Sey1p was distributed throughout the entire network, consistent with its localization in light microscopy.

Next, we tested whether Sey1p could form networks with other curvature-stabilizing proteins of the Rtn and DP1/Yop1p families. Indeed, networks were observed when Sey1p was combined with Rtn1p from *S. cerevisiae* (Fig. 4a), Rtnl1 from *D. melanogaster* (Fig. 4b), a REEP5 (DP1) homolog from *D. melanogaster* (CG8331; Fig. 4c), and REEP4 or REEP5 from *X. laevis* (Figs. 4d,e). In all these cases, network formation was only seen in the presence of GTP (Extended Data Fig. 10). Small, GTP-dependent networks were also seen when proteoliposomes containing Sey1p and *Drosophila melanogaster* Rtnl1 were analyzed by negative-stain EM (Extended Data Fig. 9d). Taken together, these results indicate that proteins of the Rtn and REEP/Yop1p families are functionally equivalent in shaping the ER network. Furthermore, given that these proteins are derived from

evolutionarily distant organisms, network formation probably does not require a specific physical interaction between Sey1p and curvature-stabilizing proteins.

Finally, we tested whether ATL, the metazoan ortholog of Sey1p, can also mediate network formation. Surprisingly, proteoliposomes containing purified *Drosophila* ATL alone formed an elaborate network upon GTP addition (Figs. 4f and Extended Data Fig. 10f). Network formation was not observed in a previous study, likely because the sample was too dilute[16]. As before, network maintenance required continuous membrane fusion; when GTPγS was added to a preformed network, it rapidly disassembled (Fig. 4g). Lowering the ATL concentration reduced network formation, but did not make it dependent on curvature-stabilizing proteins (not shown). These results suggest that ATL not only mediates fusion, but also stabilizes high membrane curvature. To test this idea, we used a fusion-defective ATL mutant (ATL^{K51A})[11] that on its own no longer formed a network (Fig. 4h). However, when co-reconstituted with Sey1p, ATL^{K51A} supported GTP-dependent network formation, indicating that it retained its curvature-stabilizing activity (Fig. 4i). *In vivo*, ATL probably only mediates fusion, while the more abundant Rtn and REEP/Yop1p proteins stabilize curvature. Because Sey1p cannot form networks on its own, it might have a lower curvature-stabilizing activity than ATL. However, it is also possible that it does not reach sufficiently high concentrations in our reconstituted vesicles, as flotation experiments show it is less efficiently incorporated into liposomes (Extended Data Fig. 3m,n). Interestingly, the network formed with ATL alone could not be visualized by EM, likely because the tubules did not survive the harsh negative-staining protocol (Fig. 3e). In contrast, networks were visible when the proteoliposomes contained both ATL and *S. cerevisiae* Yop1p (Fig. 3f,g) or ATL and *D. melanogaster* Rtnl1 (Extended Data Fig. 9e). Thus, the presence of high concentrations of curvature-stabilizing proteins makes the tubules more mechanically robust.

Our results show that a tubular ER network can be reconstituted with a surprisingly small set of membrane proteins. The network corresponds to a steady state of continuous membrane fusion and fragmentation. Fusion is mediated by the membrane-bound GTPases ATL or Sey1p, whereas fragmentation is likely caused by the curvature-stabilizing proteins of the Rtn and REEP/Yop1p families, which seem to prefer the higher membrane curvature of small vesicles to that of tubules. In a steady state network, fusion by the GTPases appears to be faster than the breakage of tubules or the shedding of small vesicles by the curvature-stabilizing proteins, explaining why tubule fission is a rare event *in vivo*. Our *in vitro* results are in agreement with recent experiments in mammalian cells, which demonstrate that ATL inactivation or overexpression of Rtn4a results in ER fragmentation[19]. Our results also show that, as in intact cells, the reconstituted network is dynamic, consisting of sliding and fusing three-way junctions. *In vivo*, these movements are caused by the attachment of the ER to the cytoskeleton or molecular motors, whereas *in vitro*, they may be due to thermal convection in conjunction with focal attachment of the network to the cover slip. We speculate that both the continuous formation and disassembly of the ER network and the dynamics of tubular junctions may allow the rapid adaptation of ER shape to different conditions. For example, it may contribute to the conversion of tubules to sheets during the cell cycle and may explain changes of ER morphology during cell differentiation. We propose that other organelles are shaped by similar principles as the ER, representing a steady state between formation and disassembly mediated by a small set of proteins.

Materials and Methods

Plasmids

Codon-optimized *D. melanogaster* (Dm) ATL (NM_001300577.1) and *S. cerevisiae* SEY1 (NM_001183584.1) were cloned into pGEX-6P-1 and pGEX-4T-3 as described previously[7,13]. Site-directed mutagenesis was used to generate the mutant DmATL^{K51A}. To generate a GFP-SEY1 fusion protein, SEY1 was cloned into the pET28b vector engineered with an N-terminal streptavidin binding protein (SBP) tag followed by a tobacco etch virus (TEV) protease cleavage site and super-folder GFP. *S. cerevisiae* (Sc) YOP1 (NM_001184125.1) and ScRTN1 (NM_001180541.3) were both cloned into the pRS426 vector with a Gal1 promoter and a CYC1 terminator. The vector also contains a N-terminal His_{14} tag and a TEV protease cleavage site. Both genes are tagged with a C-terminal sortase sequence. *D. melanogaster* reticulon-like1 (Rtnl1; NM_001169405), *X. laevis* REEP4 (codon optimized for *E. coli*; NM_001093429), and *X. laevis* REEP5 (NM_001096221.1) were cloned into the NdeI and XhoI restriction sites of a modified pET21b vector that included a C-terminal 3C protease site followed by a His_{10} tag. The *D. melanogaster* REEP homolog CG8331 (AY069293.1) was cloned into the pFastBac1 vector with a TEV protease site and a (SBP) tag at the C-terminus.

Protein expression and purification

ScYop1p and ScRtn1p were expressed and purified as C-terminal sortase fusion proteins in *S. cerevisiae*. Cells were first grown in synthetic complete media selecting for the appropriate plasmid to stationary phase to deplete glucose at 30 °C. Galactose was then added to 2% to induce the expression of the proteins at room temperature for 16 hrs. Cells were collected, washed once in water and resuspended in lysis buffer (20 mM Tris pH 7.5, 300 mM NaCl, 10% glycerol, 20 mM imidazole, 1 mM phenylmethylsulfonyl fluoride (PMSF) and protease inhibitors). Cells were lysed in a bead beater for 30 min at 4 °C. The lysate was centrifuged at low speed to clear cellular debris and unbroken cells and then at 100,000 g for 1 hr to sediment the membranes. Membranes were washed twice with lysis buffer and then solubilized in lysis buffer containing 1% n-dodecyl-β-maltoside (DDM) for 1 hr at 4 °C. Insoluble material was removed by centrifugation at 100,000 g for 1 hr and the resulting supernatant was incubated with Ni-NTA resin (Qiagen) for 1–2 hrs. Proteins were eluted using lysis buffer containing 250 mM imidazole and 0.03% DDM and incubated with TEV protease overnight at 4 °C to remove the His_{14} tag. Proteins were further purified by size-exclusion chromatography on a Superdex200 column (GE Healthcare) and concentrated by ultrafiltration (Amicon Ultra, EMD Millipore). Absorbance at 280 nm was used to determine concentrations of the all the proteins purified using DDM.

D. melanogaster ATL, *S. cerevisiae* Sey1p, GFP-Sey1p, *D. melanogaster* Rtnl1, *X. laevis* REEP4, and *X. laevis* REEP5 were expressed in *E. coli* BL21-CodonPlus (DE3)-RIPL (Agilent). Expression was induced at OD_{600} ~ 0.6–1.0 with 250 μM isopropyl-β-D-thiogalactopyranoside (IPTG) at 16 °C for 16–18 hrs. The lysis buffer used for GFP-Sey1p did not contain glycerol, which interferes with the binding of SBP tag to the streptavidin agarose resin. Cells were lysed either by sonication or through high-pressure homogenization in an M-110P microfluidizer (Microfluidics). The subsequent purification

steps were similar to what was described for ScYop1p and ScRtn1p purification with some minor differences. Membranes were washed once with buffer and then solubilized for 1 hr with 1% DDM, except for DmATL, which was solubilized with 1% Triton X-100 (TX-100). The clarified supernatant was passed over the appropriate affinity-resin for 1–2 hrs to bind the tagged protein—Ni-NTA resin in the case of REEP4, REEP5, and DmRtnl1; glutathione agarose in the case of Sey1p and DmATL; streptavidin agarose resin in the case of GFP-Sey1p. The proteins were eluted from the affinity-resin by on-column cleavage of the affinity tags. 3C protease was used to cut off all tags except in the case of Sey1p and GFP-Sey1p, for which thrombin and TEV protease was used, respectively. All proteins were further purified by size-exclusion chromatography. For DmATL, which was purified in TX-100, protein concentration was measured using a 660 nm Protein Assay (Thermo Scientific Pierce).

The pFastBac1 vector containing the CG8331-SBP gene was first transformed into DH10Bac cells to obtain the recombinant bacmid. The isolated bacmid was used to infect Sf9 insect cells and P0 virus was collected after 4–5 days. The viral stock was amplified to the P3 virus stage. The expression of the fusion protein was examined after each amplification step by immunostaining the infected Sf9 cells with a SBP antibody (Millipore). The P3 virus was used to infect 500 ml of Sf9 insect cells and cells were collected 48 hrs post-infection at 1,000 g for 10 min. Cells were broken by passing them through a dounce homogenizer fifty times and the homogenate was centrifuged at 5,000 rpm for 15 min to remove unbroken cells and debris. The subsequent purification steps were performed in TX-100 and the SBP tag was removed by on-column TEV cleavage, as described above.

Labeling of *S. cerevisiae* Yop1p with Alexa Fluor 647 dye

Purified ScYop1p was mixed with Alexa Fluor 647 NHS ester dye (Thermo Fischer Scientific) at a 1:1 protein:dye molar ratio and incubated at room temperature for 1 hr. The labeling reaction was quenched by addition of 100 mM Tris pH 8.0. After an incubation of 1 hr at 4 °C, excess dye was removed by passing the sample over Sephadex G-50 resin (GE healthcare). The labeled protein was collected and concentrated by ultrafiltration using a 50,000 MW cut-off filter (Amicon Ultra, EMD Millipore). The labeling efficiency was ~50%, as calculated by comparing the absorbance of the protein at 280 nm and the absorbance of the dye using the pre-configured “Proteins & Labels” function on a Nano Drop 2000c Spectrophotometer (Thermo Scientific).

Preparation of liposomes

All lipids were obtained as chloroform stocks from Avanti Polar Lipids. For fusion assays, donor and acceptor liposomes had a lipid composition as described previously[24] with minor modification. Donor liposomes consisted of 65:17:15:1.5:1.5 mole percent of 1-palmitoyl-2-oleoyl-sn-glycero-3-phosphocholine (POPC): 1,2-dioleoyl-*sn*-glycero-3-phosphoethanolamine (DOPE): 1,2-dio-leoyl-sn-glycero-3-phosphoserine (DOPS): NBD-1,2-dipalmitoyl-sn-glycero-3-phosphoethanolamine (NBD-DPPE): rhodamine-DPPE. Acceptor liposomes consisted of 65:18.5:15:1.5 mole percent of POPC:DOPE:DOPS:dansyl-DPPE. For confocal fluorescence microscopy experiments,

synthetic liposomes consisting of 65:18.5:15:1.5 mole percent of POPC:DOPE:DOPS: 1,2-dioleoyl-*sn*-glycero-3-phosphoethanolamine-N-[lissamine rhodamine B sulfonyl] (Rh-PE), or *E. coli* extract liposomes consisting of 98.5:1.5 mole percent of *E. coli* Polar Lipid Extract:Rh-PE, or *S. cerevisiae* extract liposomes consisting of 98.5:1.5 mole percent Yeast Polar Lipid Extract (*S. cerevisiae*):Rh-PE were used. For electron microscopy experiments, liposomes consisting of 60:33.4:6.6 mole percent of 1,2-dioleoyl-*sn*-glycero-3-phosphocholine (DOPC):DOPE:DOPS were used.

All chloroform lipid mixtures were first dried under a nitrogen stream and then under vacuum overnight to yield a thin lipid film. These lipid films were hydrated in A100 buffer (25 mM HEPES, pH 7.5, 100 mM KCl, 10% glycerol, 1 mM EDTA, 2 mM β-mercaptoethanol) and subjected to 10 freeze-thaw cycles in liquid N_2 and water at room temperature. For the fusion assay and confocal fluorescence microscopy experiments, liposomes were extruded 21 times through polycarbonate filters of 100 nm pore size using a mini-extruder (Avanti Polar Lipids) at room temperature. For the EM experiments, the liposomes were used without extrusion.

Reconstitution of protein into liposomes

Detergent-mediated reconstitution was used to integrate all proteins into liposomes as previously described[11,13,25]. Briefly, liposomes and protein were incubated together at the desired protein:lipid ratio in A100 buffer. This mixture was supplemented with DDM such that the final estimated detergent concentration was ~0.1%. The mixture was incubated at room temperature for 30 min. The detergent was then removed by four successive additions Bio-Beads SM-2 Resin (Bio-Rad) over the course of 4 hrs. Insoluble aggregates were removed by centrifugation. To examine the reconstitution efficiency, an aliquot was floated in a 0–40% w/v Nycodenz step-gradient and fractions were collected and analyzed by SDS-PAGE. To determine the orientation of proteins inserted into liposomes, equal volumes of proteoliposomes were incubated with a decreasing amounts of trypsin (0.2, 0.04, 0.008 and 0.0016 μg) in the absence or presence of 0.2% Triton-X 100 for 30 min at room temperature. Reactions were stopped by PMSF and SDS-containing protein loading dye, and analyzed by SDS-PAGE.

Lipid-mixing fusion assay

Fusion assays were performed as previously described[13] with the modifications of the lipid compositions of donor and acceptor liposomes described above. Briefly, Sey1p and Yop1p were reconstituted at the indicated protein:lipid ratios into donor and acceptor liposomes in the presence of A100 buffer containing 0.1% DDM at room temperature. Donor vesicles contained NBD-PE and rhodamine-PE. After detergent removal by Bio-Beads SM-2 Resin (Bio-Rad), samples were spun once to remove insoluble material. Lipid concentration was determined based on rhodamine or dansyl fluorescence. Donor and acceptor liposomes were mixed in a 1:3 ratio in the presence of A100 buffer containing 5 mM $MgCl_2$. Data were subsequently collected every minute using a Flexstation III (Molecular Devices) at 37 °C. Pre-fusion data were collected during the first 10 min. The average of the pre-fusion data was set as the baseline fluorescence value. Buffer or 1 mM GTP was added to the reactions and the dequenching of NBD fluorescence data caused by the fusion of donor and acceptor

vesicles was followed for 40 min. Triton-X 100 was then added to a final concentration of 2.5% and the reactions further incubated for 10 min to determine maximum fluorescence. The difference between the average of the maximum fluorescence data and the baseline value is defined as “total fluorescence”. The difference between the fusion data and the baseline value was then expressed as the percentage of the total fluorescence.

Imaging of reconstituted networks by confocal fluorescence microscopy

To test for network formation, a proteoliposome solution was supplemented with 5 mM $MgCl_2$ prior to addition of any nucleotide. Then, either 2 mM GTP, 2 mM GTPγS, or A100 buffer was added to the proteoliposome solution and the reaction was incubated for 1–2 min at room temperature. Three μl of sample was placed between two PEG-passivated No. 1.5 coverslips, which were mounted onto a metal slide and sealed with VALAP (1:1:1 mixture of vaseline, lanolin and paraffin). The coverslips were passivated with 5,000 MW polyethylene glycol (PEG) as previously described[21]. After mounting, the samples were incubated at room temperature for 10–20 min prior to imaging. All fluorescence microscopy samples were visualized using a spinning disk confocal head (CSU-X1; Yokogawa Corporation of America) with Borealis modification (Spectral Applied Research) and a quad bandpass 405/491/561/642 dichroic mirror (Semrock). The confocal was mounted on a Ti motorized inverted microscope (Nikon) equipped with a 60× Plan Apo NA 1.4 oil immersion objective or a 40× Plan Fluor NA 1.3 oil immersion objective and the Perfect Focus System for continuous maintenance of focus (Nikon). Green fluorescence images were collected using a 488-nm solid-state laser, controlled with an AOTF (Spectral Applied Research) and ET525/50 emission filter (Chroma Technology Corp.). Red fluorescence images were collected using a 561-nm solid-state laser controlled with an AOTF and ET620/60 emission filter. Far-red fluorescence images were collected using a 642-nm solid-state laser controlled with an AOTF and ET700/75 emission filter. The laser lines are combined in an LMM5 laser merge module (Spectral). All images were acquired with a cooled CCD camera (ORCA R2; Hamamatsu Photonics) controlled with MetaMorph software (version 7.0; Molecular Devices) and archived using ImageJ (National Institutes of Health). In some cases, linear adjustments were applied to enhance the contrast of images.

For network disassembly, reconstituted networks were first formed using GTP and spotted onto a passivated coverslip. GTPγS at the desired concentration was added to the solution on the coverslip immediately prior to sandwich-sealing the sample with VALAP and imaging. The time between GTPγS addition and taking the first image was about 1.5 min.

Imaging of reconstituted networks by negative-stain electron microscopy

For negative stain electron microscopy analysis, samples were prepared as previously described[9]. Briefly, 5 μl of proteoliposome solution was mixed with 7.5 μl of buffer A100 supplemented with 5 mM $MgCl_2$. Buffer or 1 mM GTP were then added and the reactions incubated for 20 min at room temperature. Subsequently, 0.5 μl of sample was mixed with 4.5 μl of buffer A100 and added to a glow-discharged carbon-coated copper grid (Pelco, Ted Pella Inc.) for 1 min. Excess sample was then blotted off with filter paper, the grids washed twice with deionized water, and then stained twice with freshly prepared 1% uranyl acetate. Images were collected at room temperature using a conventional transmission electron

microscope JEOL 1200EX equipped with a Tungsten filament and operated at an acceleration voltage of 80 kV. All images were acquired using an AMT 2kCCD camera.

ER network formation with *Xenopus* egg extracts

The interphase ER network was formed using the crude *Xenopus* egg extracts as described previously[21]. The network was stained with $DiOC_{18}$ and visualized by a spinning-disk confocal microscope.

Representative images

Images shown are representative of all images collected. For Figure 1, images are representative of **a,** 98 (left) and 108 (right), **b,** 15, **c,** 108 **d,** 30 **e,** 10, **f,** 30 total images captured. For Figure 2, images are representative of **a,** 18 (left) and 30 (right), **b,** total 36 images captured. For Figure 3, Images are representative of **a,** 21 (left) and 25 (right), **b,** 7 (left) and 17 (right), **c,** 12 (left) and 15 (right), **d,** 78 (left) and 52 (right), **e,** 10 (left) and 10 (right), **f,** 9 (left) and 23 (right), **g,** 5 (left) and 20 (right) total images captured. For Figure 4, images are representative of **a,** 20, **b,** 23, **c,** 21, **d,** 27, **e,** 15, **f,** 20, **g,** 20, **h,** 18, **i,** 32 total images captured. For Extended Data Figure 5, images are representative of 108 total images captured. For Extended Data Figure 6, images are representative of **a,** 11 (left) and 10 (right), **b,** 15 and **c,** 10 total images captured. For Extended Data Figure 7, images are representative of **a,** 15 (left) and 25 (right), **b,** 13 (left) and 20 (right) total images captured. For Extended Data Figure 8, images are representative of **a,** 10 (left) and 25 (right), **b,** 12 (left) and 34 (right) total images captured. For Extended Data Figure 9, images are representative of **a,** 25, **b,** 17 **c,** 17 **d,** 6 (left) and 12 (right), **e,** 5 (left) and 6 (right) total images captured. For Extended Data Figure 10, images are representative of **a,** 18, **b,** 10, **c,** 14, **d,** 17, **e,** 13, **f,** 11, **g,** 12, **h,** 10 total images captured.

Data Availability

Source gels for Extended Data Figures 2 and 3 are provided with the paper as SI (Supplementary Figure 1). The authors declare that all the data supporting the findings of this study are available within the paper and its supplementary information files with the exception of the low ATL concentration experiments, which are available upon request.

Extended Data

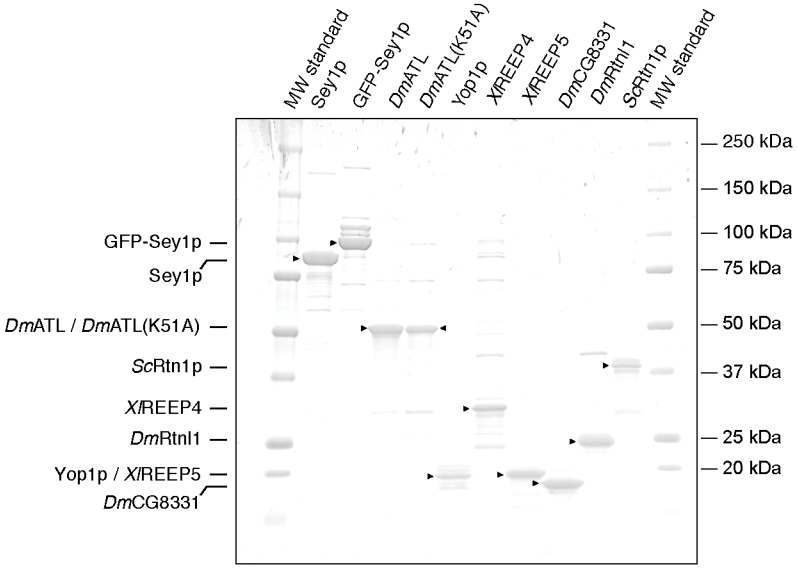

Extended Data Figure 1. Purity of ER-shaping proteins used in reconstitution experiments
The indicated proteins were purified and subjected to SDS-PAGE and Coomassie blue staining.

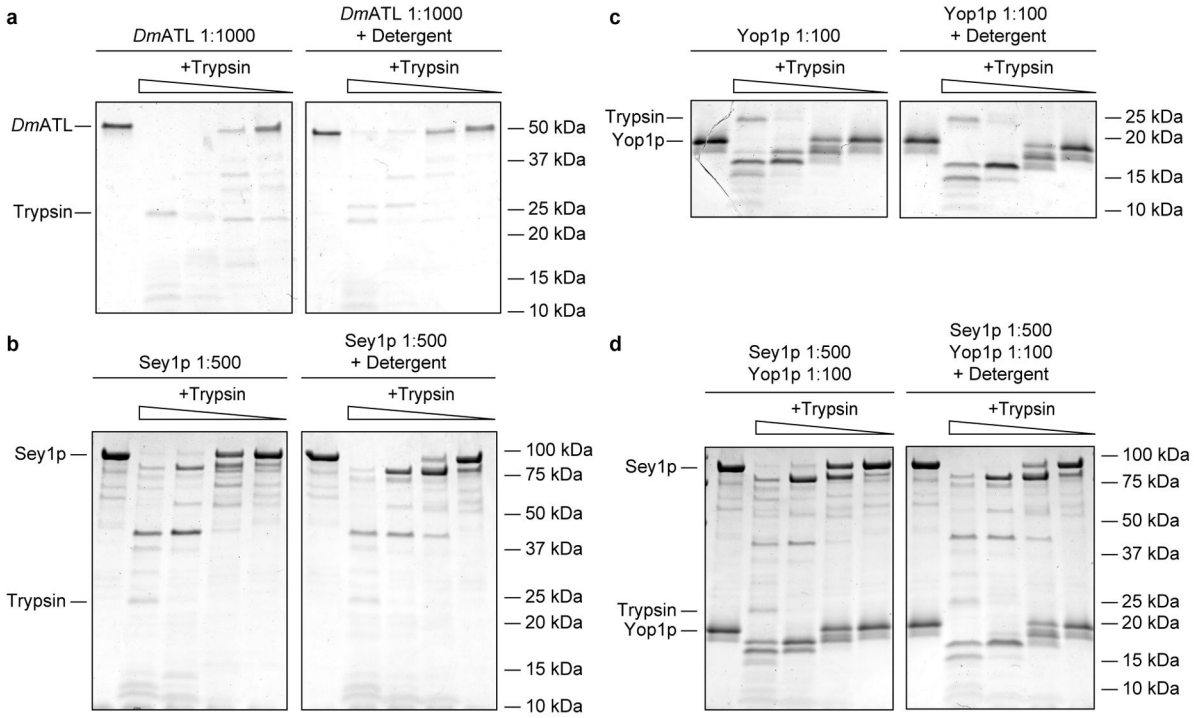

Extended Data Figure 2. Orientation of proteins after reconstitution into liposomes
a, *D. melanogaster* ATL was reconstituted into rhodamine-PE labeled liposomes at a protein:lipid ratio of 1:1000. The vesicles were incubated with decreasing amounts of

trypsin in the absence (left) or presence (right) of 0.2% Triton-X 100 for 30 min at room temperature. Samples were analyzed by SDS-PAGE and Coomassie blue staining. **b**, As in **a**, but with *S. cerevisiae* Sey1p at a protein:lipid ratio of 1:500. **c**, As in **a**, but with *S. cerevisiae* Yop1p at a protein:lipid ratio of 1:100. **d**, As in **a**, but with Sey1p and Yop1p at protein:lipid ratios of 1:500 and 1:100, respectively. For gel source data, see Supplementary Fig. 1.

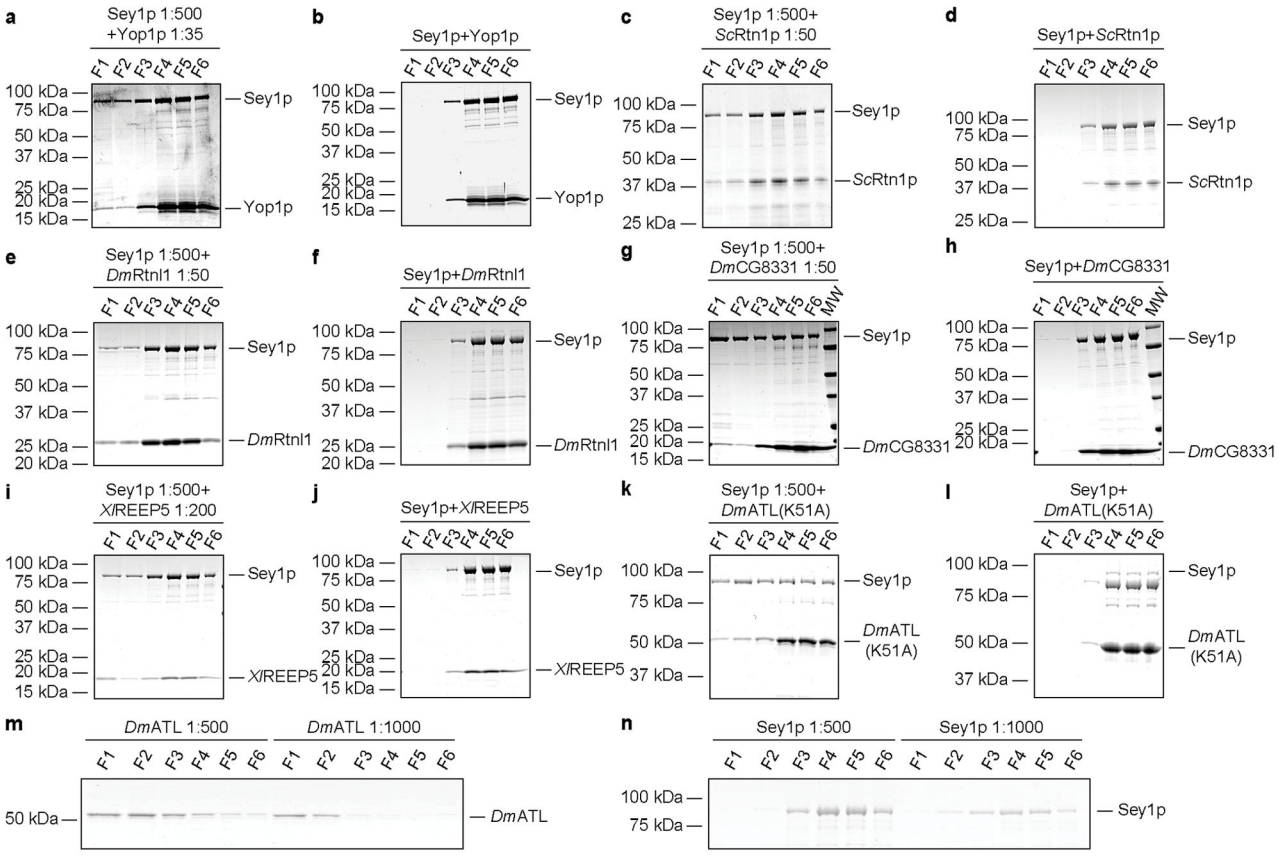

Extended Data Figure 3. Flotation of proteoliposomes generated with Sey1p and curvature-stabilizing proteins

a, *S. cerevisiae* Sey1p and Yop1p were co-reconstituted into rhodamine-PE labeled liposomes at protein:lipid ratios of 1:500 and 1:35, respectively. The samples were centrifuged in a Nycodenz gradient, and fractions (F1–F6) were collected from the top and analyzed by SDS-PAGE and Coomassie blue staining. **b**, As in **a**, but with proteins only in the presence of 0.03% DDM. **c**, As in **a**, but with proteoliposomes containing *S. cerevisiae* Sey1p and Rtn1p at protein:lipid ratios of 1:500 and 1:50, respectively. **d**, As in **c**, but with proteins only in the presence of 0.03% DDM. **e**, As in **a**, but with proteoliposomes containing Sey1p and *D. melanogaster* Rtn1p at protein:lipid ratios of 1:500 and 1:50, respectively. **f**, As in **e**, but with proteins only in the presence of 0.03% DDM. **g**, As in **a**, but with proteoliposomes containing Sey1p and *D. melanogaster* CG8331 at protein:lipid ratios of 1:500 and 1:50, respectively. **h**, As in **g**, but with proteins only in the presence of 0.03% DDM. **i**, As in **a**, but with proteoliposomes containing Sey1p and *X. laevis* REEP5 at

protein:lipid ratios of 1:500 and 1:200, respectively. **j**, As in **i**, but with proteins only in the presence of 0.03% DDM. **k**, As in **a**, but with proteoliposomes containing Sey1p and *D. melanogaster* ATL^{K51A} at protein:lipid ratios of 1:500 and 1:100, respectively. **l**, As in **k**, but with proteins only in the presence of 0.03% DDM. **m,** As in **a**, but with proteoliposomes containing *D. melanogaster* ATL at protein:lipid ratios of 1:500 or 1:1000. **n,** As in **a**, but with proteoliposomes containing *S. cerevisiae* Sey1p at protein:lipid ratios of 1:500 or 1:1000. For gel source data, see Supplementary Fig. 1.

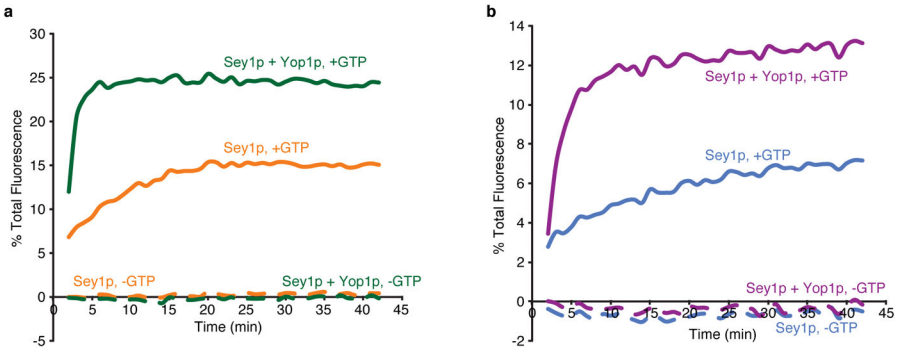

Extended Data Figure 4. Fusion activity of Sey1p-containing proteoliposomes

a, Proteoliposomes were generated with either *S. cerevisiae* Sey1p alone (protein:lipid ratio of 1:500) or with Sey1p and *S. cerevisiae* Yop1p (protein:lipid ratios of 1:500 and 1:100, respectively). Donor vesicles contained NBD-PE and rhodamine-PE. Following addition of 1 mM GTP, fusion with unlabeled acceptor vesicles was measured by dequenching of the NBD fluorescence. Controls were performed in the absence of GTP. **b,** As in **a**, but with Sey1p and Yop1p at protein:lipid ratios of 1:1000 and 1:200, respectively. Each curve corresponds to the mean of three biological replicates.

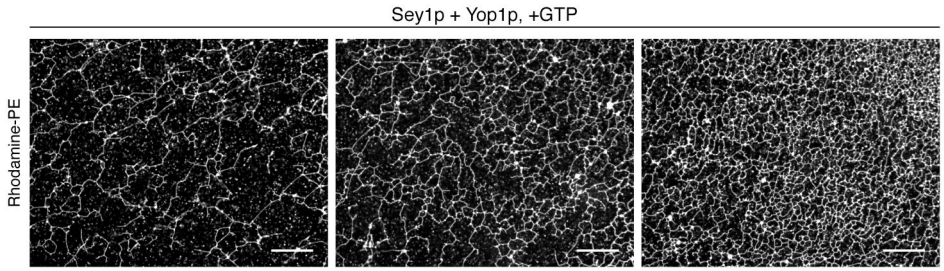

Extended Data Figure 5. Reconstituted networks display heterogeneity

S. cerevisiae Sey1p and Yop1p were incorporated into rhodamine-PE labeled liposomes at protein:lipid ratios of 1:500 and 1:35, respectively. The proteoliposomes were incubated with 2 mM GTP, spotted on a cover slip, and imaged with a fluorescence microscope. Shown are different areas from the same coverslip. Note that the networks differ with respect to the density of three-way junctions and length of tubules. Scale bars = 20 μm.

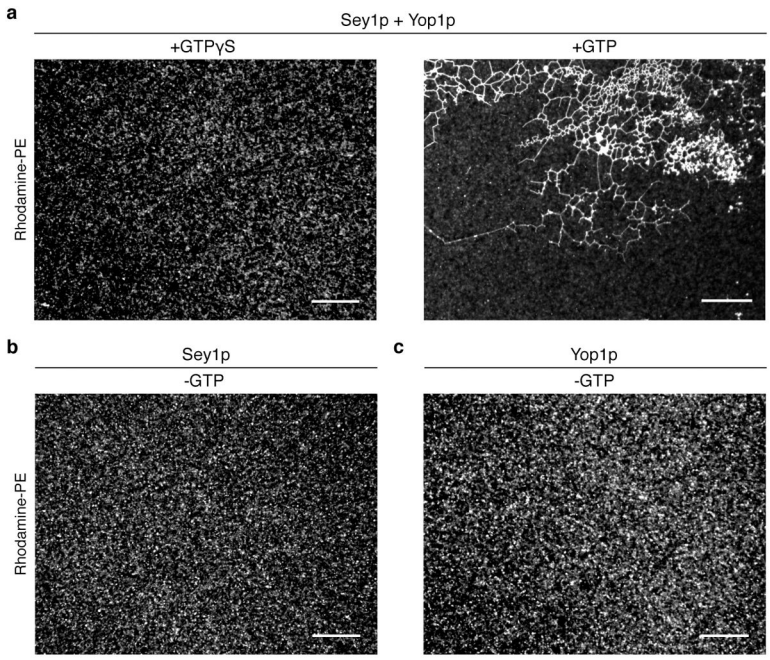

Extended Data Figure 6. Control experiments for network formation

a, *S. cerevisiae* Sey1p and Yop1p were co-reconstituted into rhodamine-PE labeled liposomes at protein:lipid ratios of 1:500 and 1:35, respectively. The proteoliposomes were incubated with either 2 mM GTP or GTPγS and visualized by fluorescence microscopy. **b**, Proteoliposomes containing only *S. cerevisiae* Sey1p at a protein:lipid ratio of 1:500 were incubated in the absence of GTP. The same sample is shown incubated with GTP in Fig. 1d. **c,** As in **b**, but with proteoliposomes containing only *S. cerevisiae* Yop1p at a protein:lipid ratio of 1:35. The same sample is shown incubated with GTP in Fig. 1e. Scale bars = 20 μm.

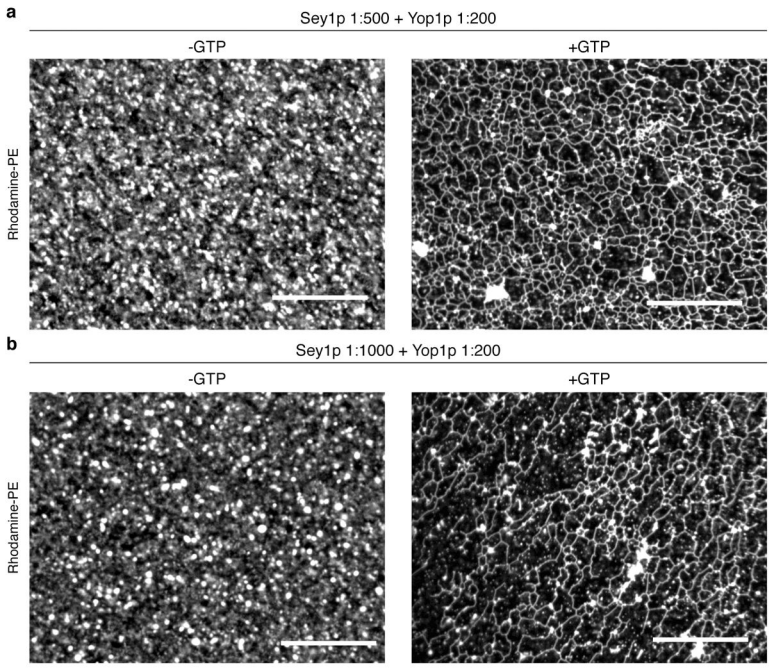

Extended Data Figure 7. Network formation with different concentrations of Yop1p and Sey1p

a, *S. cerevisiae* Sey1p was co-reconstituted with *S. cerevisiae* Yop1p into rhodamine-PE labeled liposomes at protein:lipid ratios of 1:500 and 1:200, respectively (instead of the usual 1:500 and 1:35 ratios). The proteoliposomes were incubated with or without 2 mM GTP and visualized by fluorescence microscopy. **b,** As in **a**, but with protein:lipid ratios of 1:1000 and 1:200, respectively. Scale bars = 20 μm.

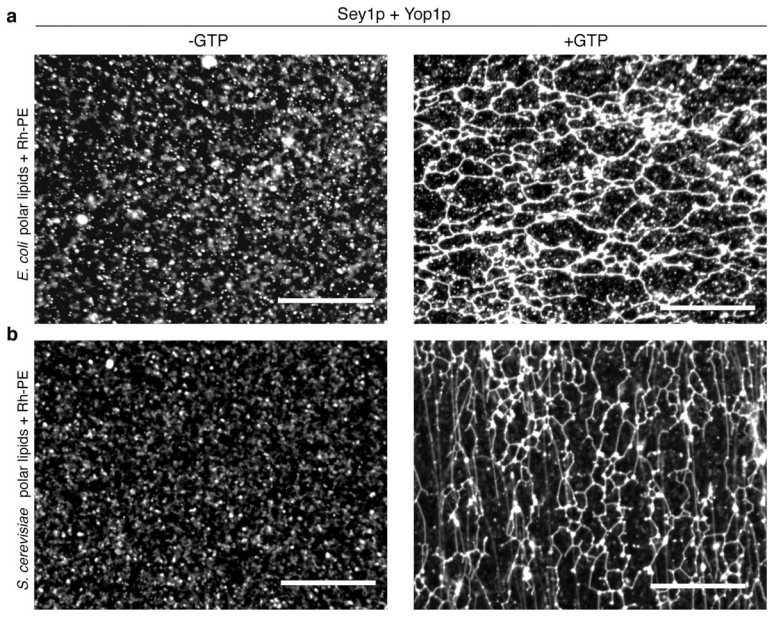

Extended Data Figure 8. Tubular network formation with different lipid compositions

a, *S. cerevisiae* Sey1p and Yop1p were co-reconstituted into rhodamine-PE labeled liposomes at protein:lipid ratios of 1:500 and 1:35, respectively. The liposomes were generated with a polar lipid extract from *E. coli*. The proteoliposomes were incubated with or without 2 mM GTP and visualized with a fluorescence microscope. **b,** As in **a,** but with liposomes generated with a polar lipid extract from *S. cerevisiae*. Scale bars = 20 μm.

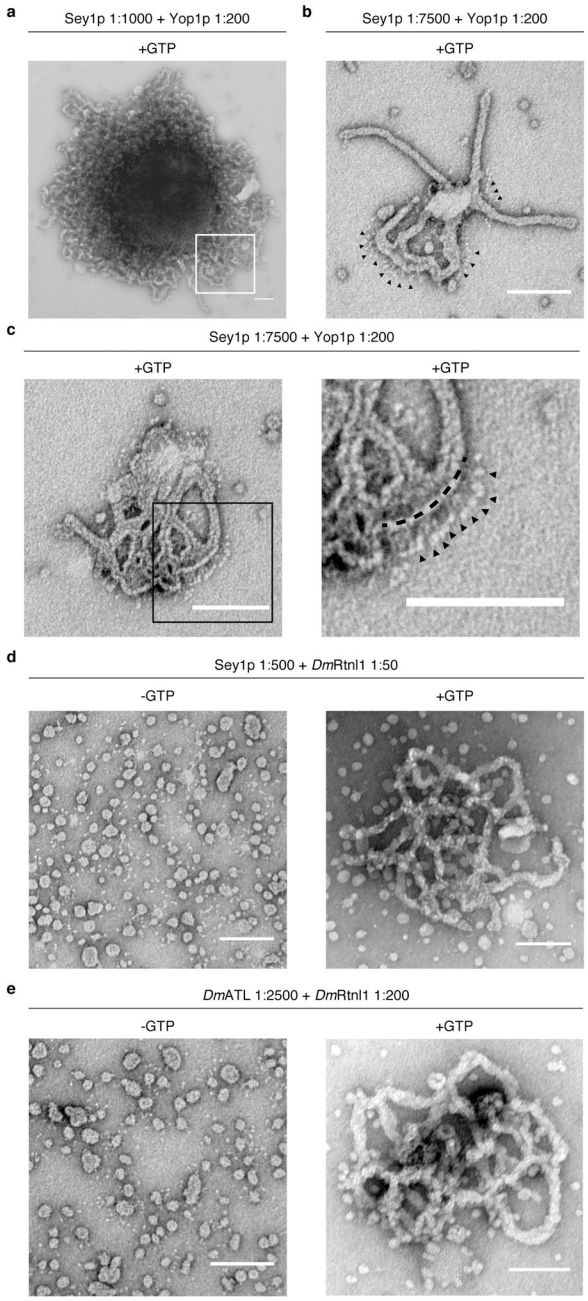

Extended Data Figure 9. Sey1p-containing networks visualized with negative-stain EM

a, *S. cerevisiae* Sey1p and Yop1p were co-reconstituted into liposomes at protein:lipid ratios of 1:1000 and 1:200, respectively. The samples were incubated with 1 mM GTP and

visualized by EM after staining with uranyl acetate. The boxed area of this network is shown enlarged in Fig. 3a. **b**, As in **a**, but with Sey1p and Yop1p at protein:lipid ratios of 1:7500 and 1:200, respectively. Black arrowheads indicate Sey1p molecules. **c**, As in **b**, showing another area (left). Boxed area is shown enlarged (right) with black arrowheads indicating Sey1p molecules and the dotted black line traces approximate plane of the lipid bilayer. **d,** As in **a**, but with Sey1p and *D. melanogaster* Rtnl1 at protein:lipid ratios of 1:500 and 1:50, respectively, in the absence or presence of 1 mM GTP. **e**, As in **a**, but with *D. melanogaster* ATL *D. melanogaster* Rtnl1 at protein:lipid ratios of 1:2500 and 1:200, respectively, in the absence or presence of 1 mM GTP. Scare bars = 100 nm.

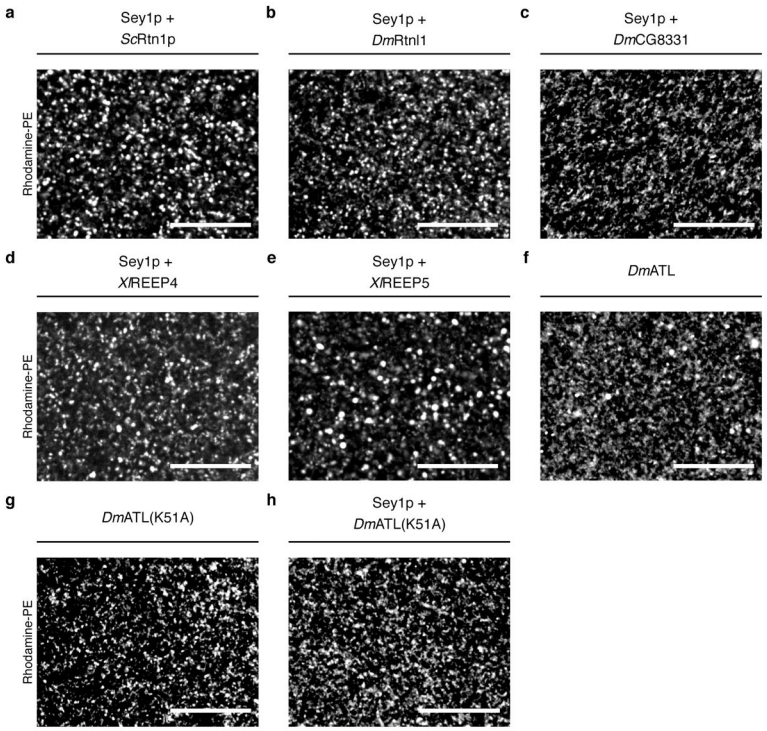

Extended Data Figure 10. Network formation with different membrane-fusing and curvature-stabilizing proteins requires GTP hydrolysis

The samples shown in Fig. 4 were incubated without GTP. Scale bars = 20 μm.

Supplementary Material

Refer to Web version on PubMed Central for supplementary material.

Acknowledgments

We thank Hanna Tukachinsky for help with protein purifications, Misha Kozlov for stimulating discussions, Andrea Daga for material, the Nikon Imaging Center at Harvard Medical School, the Harvard Medical School EM facility, and the ICCB Longwood Screening Facility for help. We thank Misha Kozlov, Junjie Hu, and Hanna Tukachinsky for critical reading of the manuscript. R.E.P. is supported by NIGMS T32 GM008313 training grant. S.W. is supported by a fellowship from the Charles King Trust. T.A.R. is a Howard Hughes Medical Institute Investigator.

References

1. Goyal U, Blackstone C. Untangling the web: mechanisms underlying ER network formation. Biochimica et biophysica acta. 2013; 1833:2492–2498. [PubMed: 23602970]
2. English AR, Voeltz GK. Endoplasmic reticulum structure and interconnections with other organelles. Cold Spring Harbor perspectives in biology. 2013; 5:a013227. [PubMed: 23545422]
3. Chen S, Novick P, Ferro-Novick S. ER structure and function. Current opinion in cell biology. 2013; 25:428–433. [PubMed: 23478217]
4. Zhang H, Hu J. Shaping the Endoplasmic Reticulum into a Social Network. Trends Cell Biol. 2016; doi: 10.1016/j.tcb.2016.06.002
5. Shibata Y, Hu J, Kozlov MM, Rapoport TA. Mechanisms shaping the membranes of cellular organelles. Annu Rev Cell Dev Biol. 2009; 25:329–354. [PubMed: 19575675]
6. Hu J, et al. A class of dynamin-like GTPases involved in the generation of the tubular ER network. Cell. 2009; 138:549–561. [PubMed: 19665976]
7. Anwar K, et al. The dynamin-like GTPase Sey1p mediates homotypic ER fusion in S. cerevisiae. The Journal of cell biology. 2012; 197:209–217. [PubMed: 22508509]
8. Voeltz GK, Prinz WA, Shibata Y, Rist JM, Rapoport TA. A class of membrane proteins shaping the tubular endoplasmic reticulum. Cell. 2006; 124:573–586. [PubMed: 16469703]
9. Hu J, et al. Membrane proteins of the endoplasmic reticulum induce high-curvature tubules. Science. 2008; 319:1247–1250. [PubMed: 18309084]
10. Park SH, Zhu P-P, Parker RL, Blackstone C. Hereditary spastic paraplegia proteins REEP1, spastin, and atlastin-1 coordinate microtubule interactions with the tubular ER network. J Clin Invest. 2010; 120:1097–1110. [PubMed: 20200447]
11. Orso G, et al. Homotypic fusion of ER membranes requires the dynamin-like GTPase atlastin. Nature. 2009; 460:978–983. [PubMed: 19633650]
12. Brady JP, Claridge JK, Smith PG, Schnell JR. A conserved amphipathic helix is required for membrane tubule formation by Yop1p. Proceedings of the National Academy of Sciences of the United States of America. 2015; 112:E639–48. [PubMed: 25646439]
13. Bian X, et al. Structures of the atlastin GTPase provide insight into homotypic fusion of endoplasmic reticulum membranes. Proceedings of the National Academy of Sciences of the United States of America. 2011; 108:3976–3981. [PubMed: 21368113]
14. Byrnes LJ, Sondermann H. Structural basis for the nucleotide-dependent dimerization of the large G protein atlastin-1/SPG3A. Proceedings of the National Academy of Sciences of the United States of America. 2011; 108:2216–2221. [PubMed: 21220294]
15. Yan L, et al. Structures of the yeast dynamin-like GTPase Sey1p provide insight into homotypic ER fusion. The Journal of cell biology. 2015; 210:961–972. [PubMed: 26370501]
16. Liu TY, et al. Cis and trans interactions between atlastin molecules during membrane fusion. Proceedings of the National Academy of Sciences of the United States of America. 2015; 112:E1851–60. [PubMed: 25825753]
17. Chen S, et al. Lunapark stabilizes nascent three-way junctions in the endoplasmic reticulum. Proceedings of the National Academy of Sciences of the United States of America. 2015; 112:418–423. [PubMed: 25548161]
18. Shemesh T, et al. A model for the generation and interconversion of ER morphologies. Proceedings of the National Academy of Sciences of the United States of America. 2014; 111:E5243–51. [PubMed: 25404289]
19. Wang S, Tukachinsky H, Romano FB, Rapoport TA. Cooperation of the ER-shaping proteins atlastin, lunapark, and reticulons to generate a tubular membrane network. eLife. 2016; 5:209.
20. Zhang D, Vjestica A, Oliferenko S. The cortical ER network limits the permissive zone for actomyosin ring assembly. Curr Biol. 2010; 20:1029–1034. [PubMed: 20434336]
21. Wang S, Romano FB, Field CM, Mitchison TJ, Rapoport TA. Multiple mechanisms determine ER network morphology during the cell cycle in Xenopus egg extracts. The Journal of cell biology. 2013; 203:801–814. [PubMed: 24297752]

22. Kulak NA, Pichler G, Paron I, Nagaraj N, Mann M. Minimal, encapsulated proteomic-sample processing applied to copy-number estimation in eukaryotic cells. Nat Methods. 2014; 11:319–324. [PubMed: 24487582]

23. Lee C, Chen LB. Dynamic behavior of endoplasmic reticulum in living cells. Cell. 1988; 54:37–46. [PubMed: 3383243]

24. Faust JE, et al. The Atlastin C-terminal tail is an amphipathic helix that perturbs the bilayer structure during endoplasmic reticulum homotypic fusion. The Journal of biological chemistry. 2015; 290:4772–4783. [PubMed: 25555915]

25. Rigaud J-L, Lévy D. Reconstitution of membrane proteins into liposomes. Methods in enzymology. 2003; 372:65–86. [PubMed: 14610807]

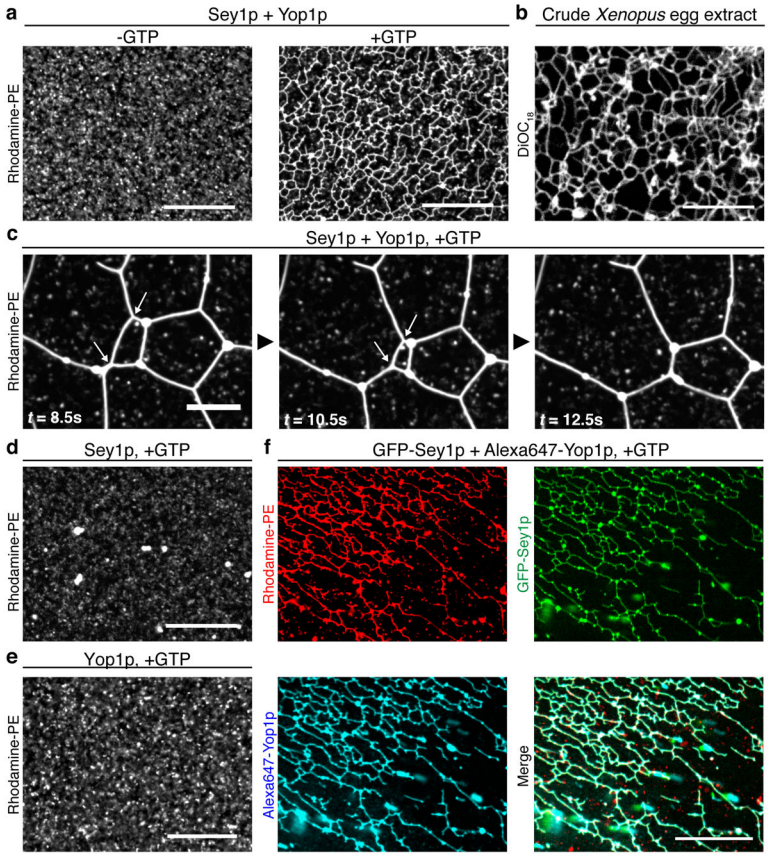

Figure 1. Co-reconstituted Sey1p and Yop1p form GTP-dependent tubular networks

a, *S. cerevisiae* Sey1p and Yop1p were co-reconstituted into rhodamine-PE labeled liposomes at protein:lipid ratios of 1:500 and 1:35, respectively, incubated without (left) or with (right) 2 mM GTP, and visualized by fluorescence microscopy. **b,** An ER network was formed with crude interphase *Xenopus* egg extract and fluorescently stained with $DiOC_{18}$. **c,** Time-lapse images of the reconstituted network (see also Supplementary Video 1). White arrows indicate sliding or fusing junctions. **d,** Proteoliposomes formed with Sey1p alone (protein:lipid ratio of 1:500) were incubated with 2 mM GTP. **e,** As in **d,** but with proteoliposomes formed with Yop1p alone (protein:lipid ratio of 1:35). **f,** As in **a,** but with GFP-labeled Sey1p and Alexa647-labeled Yop1p. Scale bars = 20 μm, except in **c** where scale bars = 10 μm.

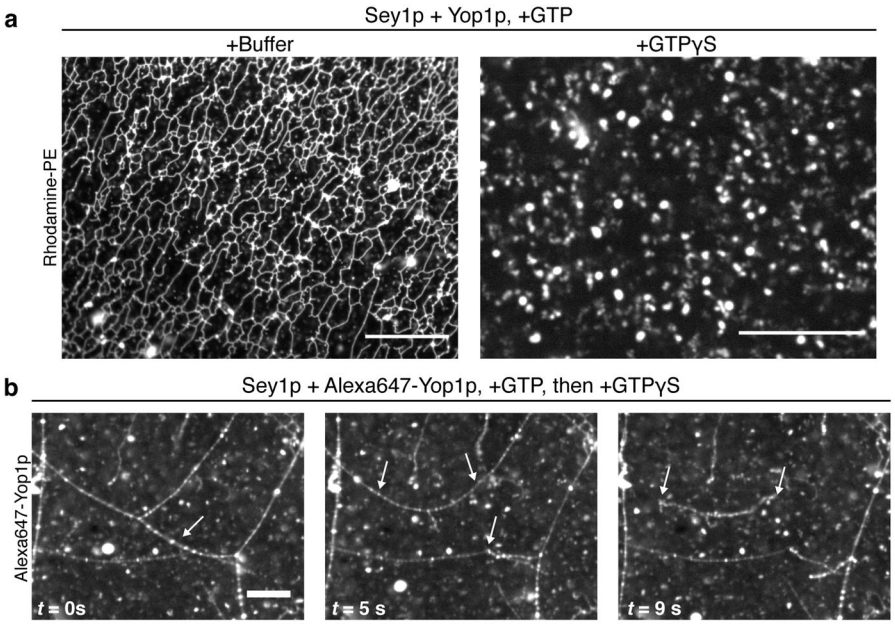

Figure 2. Network maintenance requires continuous GTP hydrolysis by Sey1p

a, *S. cerevisiae* Sey1p and Yop1p were co-reconstituted into rhodamine-PE labeled liposomes at protein:lipid ratios of 1:500 and 1:35, respectively. Network was formed by incubating proteoliposomes with 2 mM GTP. After addition of buffer (left) or 2 mM GTPγS (right), the samples were immediately analyzed. **b,** Time-lapse images after addition of 1 mM GTPγS to a preformed network formed with Sey1p and Alexa647-labeled Yop1p (see also Supplementary Video 2). Alexa647-labeled Yop1p is visualized. White arrows indicate fragmentation points. Scale bars = 20 μm for **a,** and 10 μm for **b**.

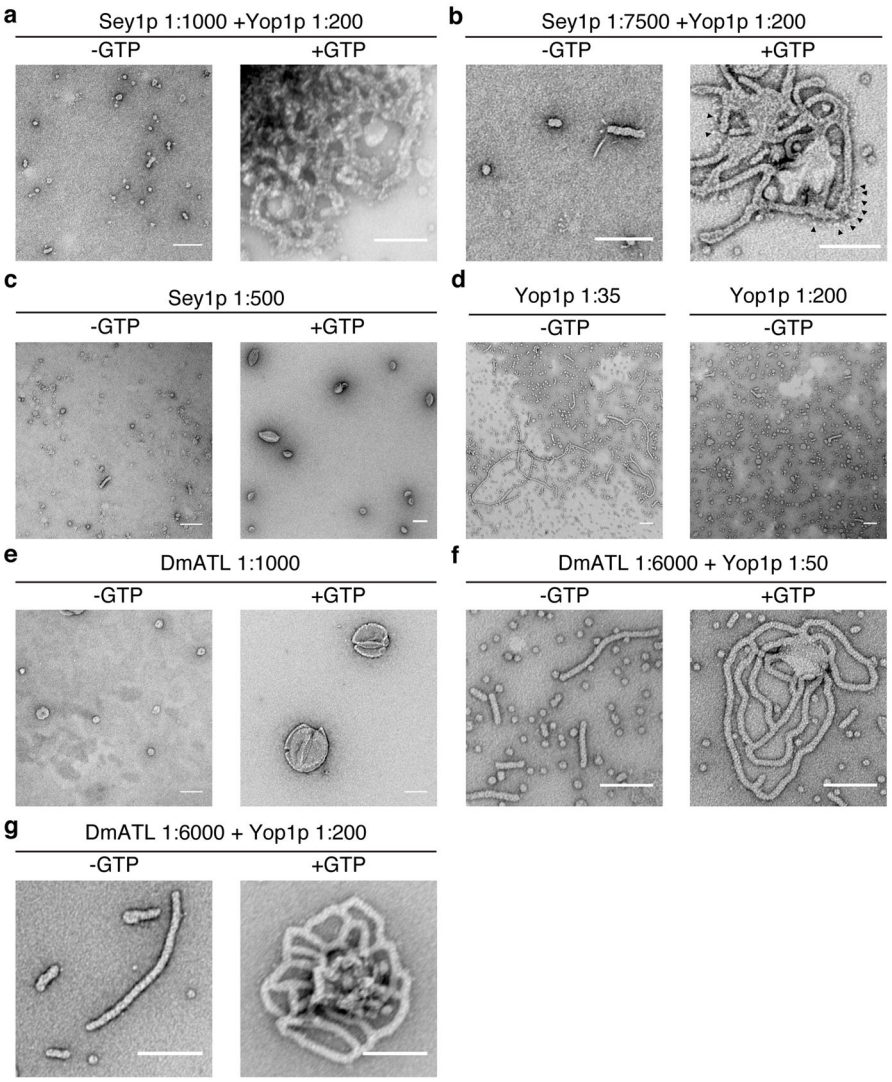

Figure 3. Visualization of reconstituted networks with negative-stain EM

a, *S. cerevisiae* Sey1p and Yop1p were co-reconstituted into liposomes at protein:lipid ratios of 1:1000 and 1:200, respectively. The samples were incubated with or without 1 mM GTP and visualized by EM after uranyl acetate staining. The figure shows a magnification of the network in Extended Data Fig. 7. **b**, As in **a**, but with Sey1p and Yop1p at protein:lipid ratios of 1:7500 and 1:200, respectively. Black arrowheads indicate Sey1p molecules. **c**, As in **a**, but with Sey1p alone at a protein:lipid ratio of 1:500. **d**, As in **a**, but with Yop1p alone at protein:lipid ratios of 1:35 and 1:200 in the absence of GTP. **e**, As in **a**, but with *D. melanogaster* ATL alone at a protein:lipid ratio of 1:1000. **f,** As in **a**, but with ATL and Yop1p co-reconstituted into liposomes at protein:lipid ratios of 1:6000 and 1:50, respectively. **g,** As in **a**, but with ATL and Yop1p at protein:lipid ratios of 1:6000 and 1:200, respectively. Scale bars = 100 nm.

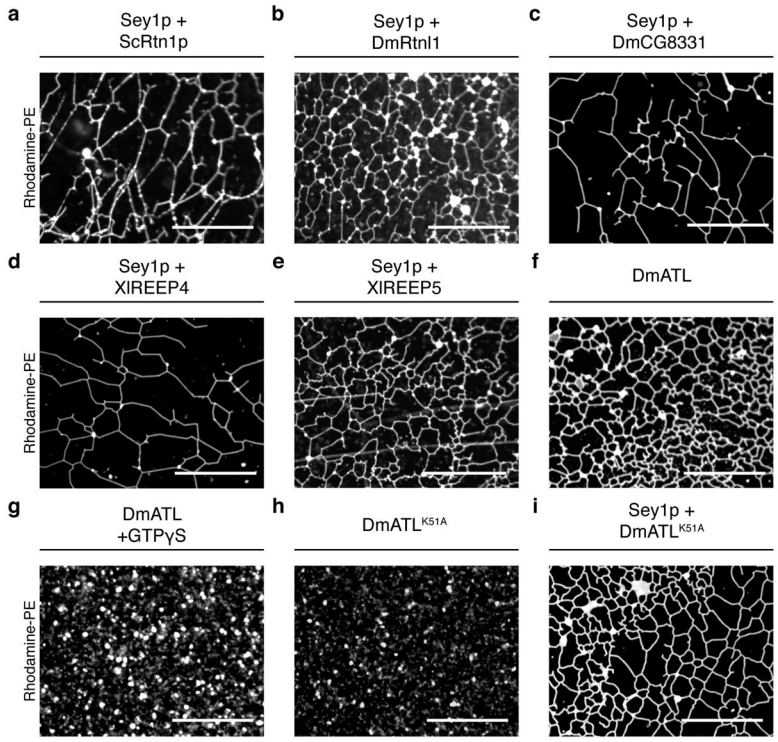

Figure 4. Networks formed with different membrane-fusing and curvature-stabilizing proteins

a, *S. cerevisiae* Sey1p was co-reconstituted with *S. cerevisiae* Rtn1p into rhodamine-PE labeled liposomes at protein:lipid ratios of 1:500 and 1:50, respectively. The proteoliposomes were incubated with 2 mM GTP and visualized by fluorescence microscopy. **b,** As in **a**, but with Sey1p and *D. melanogaster* Rtnl1. **c,** As in **a,** but with Sey1p and *D. melanogaster* REEP-homolog CG8331. **d,** As in **a**, but with Sey1p and *X. laevis* REEP4. **e,** As in **a,** but with Sey1p and *X. laevis* REEP5 (protein:lipid ratio of 1:200). **f,** Proteoliposomes formed with *D. melanogaster* ATL alone at a protein:lipid ratio of 1:1000 in the presence of 2 mM GTP. **g,** As in **f,** but 2 mM GTPγS was added after network formation. **h,** Proteoliposomes formed with fusion-defective *D. melanogaster* ATL^{K51A} alone at a protein:lipid ratio of 1:100 in the presence of 2 mM GTP. **i,** *S. cerevisiae* Sey1p and fusion-defective *D. melanogaster* ATL^{K51A} co-reconstituted at protein:lipid ratios of 1:500 and 1:100, respectively, incubated in the presence of 2 mM GTP. Scale bars = 20 μm.